Journal of Applied Analysis and Computation
Volume 5, Number 2, May 2015, 210–219
Website:http://jaac-online.com/
doi:10.11948/2015019

BIFURCATIONS AND SYNCHRONIZATION OF THE FRACTIONAL-ORDER SIMPLIFIED LORENZ HYPERCHAOTIC SYSTEM*

Yan Wang[1,2], Shaobo He[2,†], Huihai Wang[2] and Kehui Sun[1,2]

Abstract In this paper, dynamics of the fractional-order simplified Lorenz hyperchaotic system is investigated. Modified Adams-Bashforth-Moulton method is applied for numerical simulation. Chaotic regions and periodic windows are identified. Different types of motions are shown along the routes to chaos by means of phase portraits, bifurcation diagrams, and the largest Lyapunov exponent. The lowest fractional order to generate chaos is 3.8584. Synchronization between two fractional-order simplified Lorenz hyperchaotic systems is achieved by using active control method. The synchronization performances are studied by changing the fractional order, eigenvalues and eigenvalue standard deviation of the error system.

Keywords Fractional-order calculus, chaos, simplified Lorenz hyperchaotic system, bifurcation, synchronization performance, active control.

MSC(2000) 34C28, 37N35.

1. Introduction

At present, an increasingly important topic in the literature of natural and scientific areas is the fractional calculus, since it can elegantly describe various research fields, such as electrode-electrolyte polarization McAdarns etc [10], electromagnetic waves Tarasov [15], thermoelasticity Ezzat etc [4] and respiratory system Ionescu etc [6]. Due to its potential applications, many fractional-order dynamical systems have been reported, such as fractional-order Lorenz system Xu etc [16], the hybrid optical system Abdelouahab etc [1], the fractional-order neural networks system Kaslik etc [8], the fractional-order phytoplankton model Javidi [7] and the fractional-order autonomous nonlinear system Ahmad etc [2].

Meanwhile, chaos synchronization of fractional-order system is also a hot topic for its practical application, and it is a critical technique in information encryption and secure communication. Many chaos synchronization schemes are proposed, such as projective synchronization Si etc [12], function synchronization Fan etc [5], adaptive control method Zhang etc [17], linear control method Kuntanapreeda etc [9], sliding mode control method Chen [3] and active control technique Radwan

†The corresponding author. Email address: heshaobo_123@163.com (S. He)
[1]School of Physics Science and Technology, Xinjiang University, 830046, Urumqi, China
[2]School of Physics and Electronics, Central South University, 410083, Changsha, China
*The authors were supported by the National Natural Science Foundation of China (61161006 and 61073187) and the Fundamental Research for Central Universities of Central South University (2013zzts154 and 2014zzts010).

etc [11]. Here active control method is chosen to synchronize two fractional-order hyperchaotic systems.

In this paper, the dynamical behaviors of the fractional-order simplified Lorenz hyperchaotic system are investigated numerically. Furthermore, synchronization for this system is studied. This article is organized as follows. In Section 2, the fractional-order simplified Lorenz hyperchaotic system is presented. In Section 3, bifurcations, phase portraits and Poincaré sections are chosen to describe the system's dynamical behaviors with the variation of derivative order q and system parameters c and k, respectively. In Section 4, synchronization of the fractional-order system is investigated, and the factors that affect the synchronization time are analyzed. Finally, conclusions are summarized.

2. The fractional-order simplified Lorenz hyperchaotic system mode

The simplified Lorenz hyperchaotic system is investigated by Sun etc [13], which is described as

$$\begin{aligned} \dot{x} &= 10(y-x), \\ \dot{y} &= (24-4c)x - xz + cy + u, \\ \dot{z} &= xy - \frac{8}{3}z, \\ \dot{u} &= -kx, \end{aligned} \tag{2.1}$$

where x, y, z, u are state variables, c and k are system parameters. When $c = -1$, $k = 5$, the Lyapunov exponent of system (2.1) are $\lambda_i (i = 1, 2, 3, 4)$ =(0.4259, 0.3001, 0, -14.3926), which means the system is hyperchaotic. The phase portrait is shown in Fig. 1.

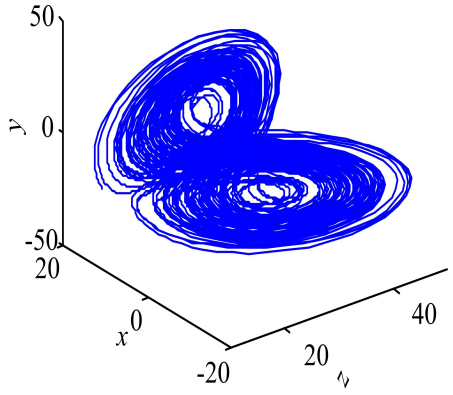

Figure 1. 3D phase diagram of system (2.1) with $c = -1$, $k = 5$.

Consider the derivational order q of system (2.1) is fractional, and the fractional-

order simplified Lorenz system has the form of

$$\begin{aligned} {}^{*}D_{t_0}^{q}x &= 10(y-x),\\ {}^{*}D_{t_0}^{q}y &= (24-4c)x - xz + cy + u,\\ {}^{*}D_{t_0}^{q}z &= xy - \frac{8}{3}z,\\ {}^{*}D_{t_0}^{q}u &= -kx, \end{aligned} \tag{2.2}$$

where ${}^{*}D_{t_0}^{q}$ is the Caputo differential operator of order $q \in (0,1]$.

3. Dynamics of the fractional-order simplified Lorenz hyperchaotic system

3.1. Numerical method for solving fractional differential equations

The Adams-Bashforth-Moulton algorithm Sun etc [14] is applied to analyze the system (2.2). The algorithm is described below. Consider the fractional differential equation with initial condition:

$$\begin{aligned} &{}^{*}D_{t_0}^{q}x(t) = f(x,x(t)), 0 \le t \le T,\\ &x^{(k)}(0) = x_0^{(k)}, k = 0,1,2,...,[q]-1, \end{aligned} \tag{3.1}$$

where $[q]$ is the first integer which is not less than q, and $x^{(k)}(t)$ is the k^{th} ordinary derivative of $x(t)$. The fractional calculus is denoted as

$$\begin{aligned} &{}^{*}D_{t_0}^{q}x(t) = J^{n-q}x^{(n)}(t),\\ &J^{\beta}x(t) = \frac{1}{\Gamma(\beta)}\int_0^t (t-\tau)^{\beta-1}x(\tau)d\tau, 0 < \beta \le 1, \end{aligned} \tag{3.2}$$

where J^{β} is the β-order Riemann-Liouville integral operator, and $\Gamma(\cdot)$ is the Gamma function. Eq. (3.2) is equivalent to the Volterra integral equation Sun etc [14]

$$x(t) = \sum_{k=0}^{[q]-1} x_0^{(k)}\frac{t^k}{k!} + \frac{1}{\Gamma(\alpha)}\int_0^t (t-\tau)^{q-1}f(\tau,x(\tau))d\tau. \tag{3.3}$$

Set $h = T/N$, $t_j = jh, j = 0,1,...,N \in Z^{+}$. Then, Eq. (3.3) can be discreted as

$$\begin{aligned} x_h(t_{n+1}) = &\sum_{k=0}^{[q]-1} x_0^{(k)}\frac{t_{n+1}^k}{k!} + \frac{h^q}{\Gamma(q+2)}f(t_{n+1},x_h^p(t_{n+1}))+\\ &\frac{h^q}{\Gamma(q+2)}\sum_{j=0}^{n}\alpha_{j,n+1}f(t_j,x_h(t_j)), \end{aligned} \tag{3.4}$$

in which

$$x_h^p(t_{n+1}) = \sum_{k=0}^{[q]-1} x_0^{(k)}\frac{t_{n+1}^k}{k!} + \frac{1}{\Gamma(q)}\sum_{j=0}^{n} b_{j,n+1}f(t_j,x_h(t_j)), \tag{3.5}$$

where

$$b_{j,n+1} = \frac{h^q}{q}[(n-j+1)^q - (n-j)^q], 0 \le j \le n, \tag{3.6}$$

$$\alpha_{j,n+1} = \begin{cases} n^{q+1} - (n-q)(n+1)^q, & j = 0, \\ (n-j+2)^{q+1} + (n-j)^{q+1} - 2(n-j+1)^{q+1}, & 1 \le j \le n, \\ 1, & j = n+1. \end{cases} \tag{3.7}$$

3.2. Bifurcations of the fractional-order system with derivative order q variation

Let $c = -1, k = 5$, the bifurcation diagram for derivative order $q \in [0.96, 1]$ is shown in Fig.2(a), where the step size of q is 0.0002. It shows system (2.2) is periodic over the range of $q \in (0.96, 0.9644)$, and as q increasing, the size of the chaotic attractor suddenly increases by a crisis bifurcation at $q = 0.9644$. To verify the chaotic behaviors, the corresponding largest Lyapunov exponent diagram is shown in Fig.2(b).

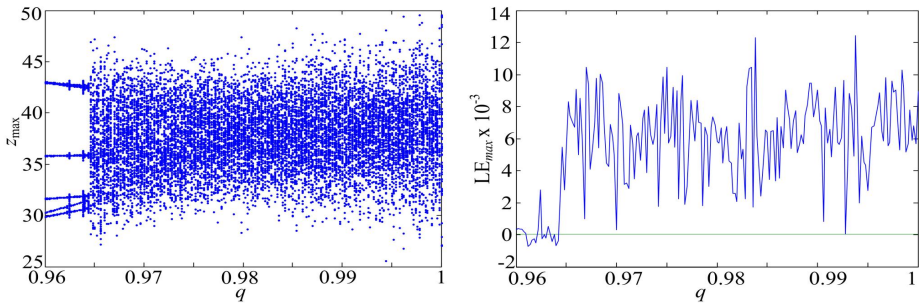

(a) Bifurcation diagram (b) Lyapunov exponent

Figure 2. Bifurcation and Lyapunov exponent with different q.

To reveal the dynamics further, phase portraits of system (2.2) on the $x-z$ plane with $q = 0.9646$ and $q = 0.9644$ are plotted in Fig. 3(a) and Fig.4(a), respectively. Fig.3(a) shows system (2.2) is chaotic as $q = 0.9646$, while system (2.2) is periodic as $q = 0.9644$. Fig.3(b) and Fig.4(b) present the Poincaré sections of $x - y$ plane in $z = 20$ with $q = 0.9646$ and $q = 0.9644$, respectively. Obviously, hierarchical dense points indicate chaos and a few discrete points mean periodic, which is in accord with the Poincaré diagrams. The corresponding frequency spectrums are displayed in Fig.3(c) and Fig.4(c). As it illustrates that when $q = 0.9644$, the system is not chaotic, and when $q = 0.9646$ the system is hyperchaotic, thus the lowest total order for system (2.2) to yield chaos is $0.9646 \times 4 = 3.8584$.

3.3. Bifurcations of the fractional-order system with c variation

Here, $q = 0.97$ and $k = 5$, let the system parameter c vary from -3 to 5 with the step size of 0.01. The bifurcation diagram in Fig.5(a) illustrates an overall perspective of system (2.2), which is different from its integer-order counterpart. The largest

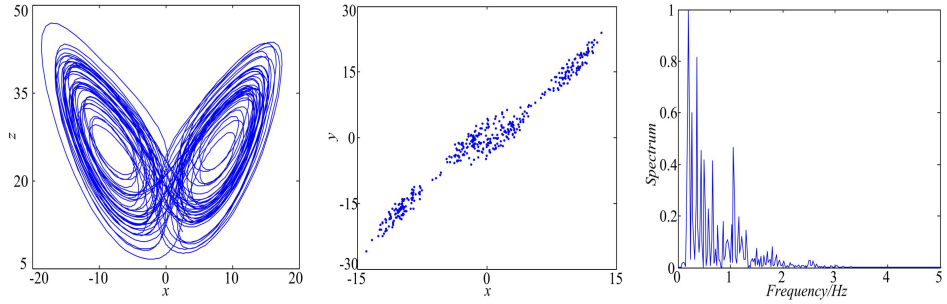

(a) Phase portrait (b) Poincaré section (c) Frequency spectrum

Figure 3. Dynamical behaviors of system (2.2) with $q = 0.9646$.

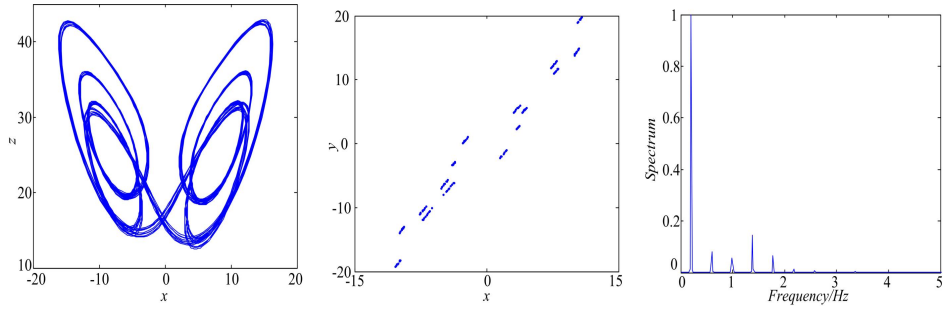

(a) Phase portrait (b) Poincaré section (c) Frequency spectrum

Figure 4. Dynamical behaviors of system (2.2) with $q = 0.9644$.

Lyapunov exponent is plotted in Fig.5 (b). The main chaotic range of the system is $c \in (-1.72, 3.47) \cup (3.66, 3.70)$, while the rest is periodic. When c decreases from 5, it displays in Fig.5(c) that the system presents a series of period-doubling bifurcations leading to a small chaotic set. With the decreasing of parameter c, a tangent bifurcation occurs at $c = 3.65$, and the system steps into periodic state again. When $c < 3.47$, the system is chaotic until a tangent bifurcation occurs at $c = -1.72$ as shown in Fig.5 (a).

3.4. Bifurcations of the fractional-order system with k variation

By fixing $q = 0.97$ and $c = -1$, varying the system parameter k from 2 to 34 with step size of 0.01, the bifurcation diagram is shown in Fig.6 (a). Chaos covers most of the range $k \in [4.31, 29]$, except $k \in [11.54, 15.50]$. To observe the dynamical behaviors, a window is separately drawn in Fig.6 (b). When k increases from 2, it runs into chaos by a tangent bifurcation at $k = 3.50$. After a while, system (2.2) is periodic again with $k \in [3.82, 4.3]$. When k decreases from 34, the system presents periodic states until it enters into chaos by the cascaded period-doubling bifurcation at $k = 29$, as shown in Fig.6(c). With a further decreasing of parameter k, the system is extracted from chaotic movement by interior crisis at $k = 15.49$.

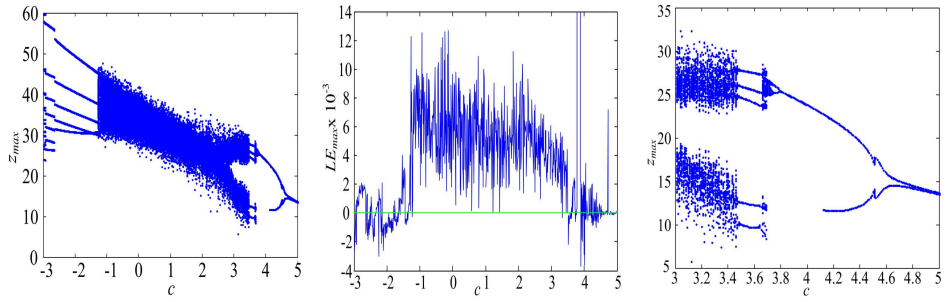

(a) Bifurcation diagram (b) largest Lyapunov exponent (c) Bifurcation diagram

Figure 5. Dynamical behaviors of system (2.2) with different c.

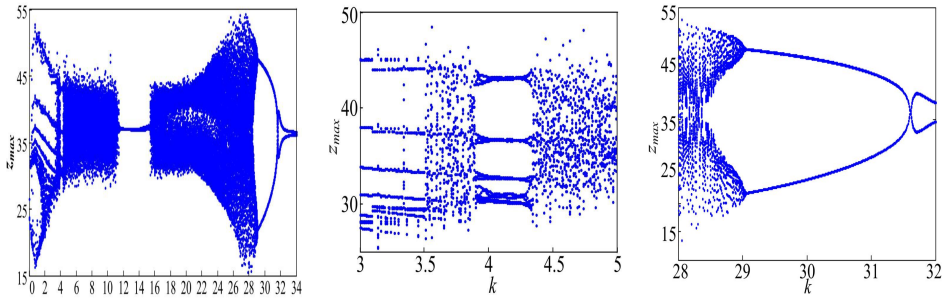

(a) $k \in (2, 34)$ (b) $k \in (3, 5)$ (c) $k \in (28, 32)$

Figure 6. Bifurcation diagram of system (2.2) with different k.

4. Synchronization of fractional-order simplified Lorenz hyperchaotic systems

Consider the fractional-order chaotic system as a master system

$$ {}^{*}D_{t_0}^{q}\mathbf{x} = \mathbf{A}\mathbf{x} + H(\mathbf{x}). \tag{4.1} $$

Then, the slave system is defined as

$$ {}^{*}D_{t_0}^{q}\mathbf{x_1} = \mathbf{A}\mathbf{x_1} + H(\mathbf{x_1}) + \mathbf{V}, \tag{4.2} $$

where $q \in (0, 1]$ is the order of the fractional derivative, $\mathbf{x}$, $\mathbf{x_1}$ are the state vectors, $H(\mathbf{x})$, $H(\mathbf{x_1})$ are the nonlinear terms of the two systems, $\mathbf{A}$ is a constant matrix and $\mathbf{V}$ is the controller. The synchronization errors are defined as $\mathbf{e} = \mathbf{x_1} - \mathbf{x}$. Then, the error system is obtained as

$$ {}^{*}D_{t_0}^{q}\mathbf{e} = \mathbf{A}\mathbf{e} + H(\mathbf{x_1}) - H(\mathbf{x}) + \mathbf{V}. \tag{4.3} $$

To synchronize the states of system (4.1) and system (4.2), a suitable controller should be chosen. Here we design the controller as

$$ \mathbf{V} = \mathbf{C}\mathbf{e} - H(\mathbf{x_1}) + H(\mathbf{x}), \tag{4.4} $$

where $\mathbf{C}$ is a constant matrix with the same size as $\mathbf{A}$. By employing this designed controller, the error system now is

$$ {}^{*}D_{t_0}^{q}\mathbf{e} = (\mathbf{C}+\mathbf{A})\mathbf{e}. \tag{4.5} $$

Under the condition $|arg(\lambda_{i(\mathbf{A}+\mathbf{C})})| > \frac{q}{2}$, system (4.1) and system (4.2) can realize synchronization.

The system (2.2) is chosen as the master system with $c = -1, k = 5$ and the Jacobian matrix $\mathbf{A}$ is obtained by linearizing the system at the equilibrium

$$ \mathbf{A} = \begin{bmatrix} -10 & 10 & 0 & 0 \\ 28 & -1 & 0 & 1 \\ 0 & 0 & -8/3 & 0 \\ -5 & 0 & 0 & 0 \end{bmatrix}. \tag{4.6} $$

Then, the slave system with the controller $\mathbf{V}$ is described as follows:

$$ \begin{bmatrix} {}^{*}D_{t_0}^{q}x_1 \\ {}^{*}D_{t_0}^{q}y_1 \\ {}^{*}D_{t_0}^{q}z_1 \\ {}^{*}D_{t_0}^{q}u_1 \end{bmatrix} = \mathbf{A}\begin{bmatrix} x_1 \\ y_1 \\ z_1 \\ u_1 \end{bmatrix} + \begin{bmatrix} 0 \\ -x_1z_1 \\ x_1y_1 \\ 0 \end{bmatrix} + \mathbf{V}. \tag{4.7} $$

So, the error system derived from system (2.2) and system (4.3) is written as

$$ {}^{*}D_{t_0}^{q}\mathbf{e} = \mathbf{A}\mathbf{e} + \begin{bmatrix} 0 \\ -x_1z_1 + xz \\ x_1y_1 - xy \\ 0 \end{bmatrix} + \mathbf{V}, \tag{4.8} $$

where $\mathbf{e} = (e_1, e_2, e_3, e_4)^T$, $e_1 = x_1 - x$, $e_2 = y_1 - y$, $e_3 = z_1 - z$, $e_4 = u_1 - u$. According to Eq. (4.4), the controller $\mathbf{V}$ becomes

$$ \mathbf{V} = \begin{bmatrix} 0 \\ x_1z_1 - xz \\ -x_1y_1 + xy \\ 0 \end{bmatrix} + \mathbf{C}\mathbf{e}. \tag{4.9} $$

Next step is to design an appropriate matrix $\mathbf{C}$ which stabilizes the system so that $\mathbf{e}$ converges to zero as time t tends to infinity. There is not a unique choice for such matrix $\mathbf{C}$. For example, when matrix $\mathbf{C}$ is set as

$$ \mathbf{C} = \begin{bmatrix} 0 & -10 & 0 & 0 \\ -28 & -9 & 0 & -1 \\ 0 & 0 & -22/3 & 0 \\ 5 & 0 & 0 & -10 \end{bmatrix}, \tag{4.10} $$

the error system is changed to

$$ {}^{*}D_{t_0}^{q}\mathbf{e} = (\mathbf{A}+\mathbf{C})\mathbf{e} = \begin{bmatrix} -10 & 0 & 0 & 0 \\ 0 & -10 & 0 & 0 \\ 0 & 0 & -10 & 0 \\ 0 & 0 & 0 & -10 \end{bmatrix}\mathbf{e}. \tag{4.11} $$

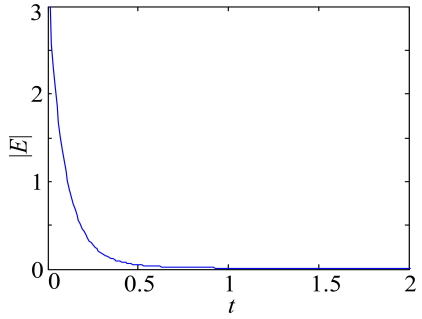

Figure 7. Error curve of synchronization system with $q = 0.97$.

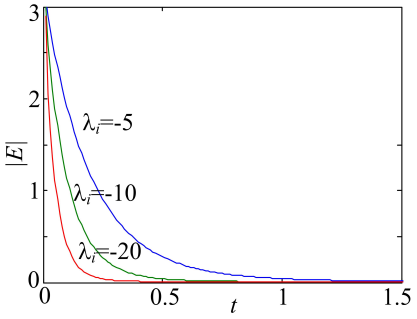

Figure 8. Error curves of the synchronized system with different λ.

All the four eigenvalues of the system are negative, the error curves of synchronization system with $q = 0.97$ is presented in Fig.7, where $|E| = (e_1^2+e_2^2+e_3^2+e_4^2)^{1/2}$. The synchronization time with different q are obtained as displayed in Table 1, where the synchronization precision is 10^{-3}. It indicates that the synchronization time is decreasing with the increasing of q.

Table 1. Synchronization time with different q.

Derivative order q	Synchronization time (s)
0.96	2.49
0.97	1.88
0.98	1.24
0.99	0.84
1.00	0.63

Furthermore, it is found that when all the eigenvalues are negative, the eigenvalues $\lambda_{i(\mathbf{A}+\mathbf{C})}$ also affect the synchronization time. Here, we set $q = 0.98$. Some data is collected to verify the point as displayed in Table 2. Obviously, when the sum of all the eigenvalues is the same, the smaller the standard deviation of the eigenvalues $\lambda_{i(\mathbf{A}+\mathbf{C})}$ is, the shorter the synchronization time is.

Table 2. Synchronization time with the standard deviation of $\lambda_{i(\mathbf{A}+\mathbf{C})}$.

$\lambda_{i(\mathbf{A}+\mathbf{C})}$	Standard deviation of $\lambda_{i(\mathbf{A}+\mathbf{C})}$	Synchronization time (s)
$(-0.5, -0.5, -1, -38)$	18.6680	18.59
$(-5, -4, -8, -23)$	8.8318	2.14
$(-16, -12, -6, -6)$	4.8990	1.96
$(-8, -12, -8, -12)$	2.3094	1.25
$(-10, -10, -10, -10)$	0.0000	1.24

The case that all the eigenvalues are the same is also studied. Choosing $\lambda_{i(\mathbf{A}+\mathbf{C})}$ = (-5, -5, -5, -5), $\lambda_{i(\mathbf{A}+\mathbf{C})}$ = (-10, -10, -10, -10), and $\lambda_{i(\mathbf{A}+\mathbf{C})}$ = (-20, -20, -20, -20) as examples to reveal the rules, the result is depicted in Fig.8. It exhibits that the smaller the eigenvalues $\lambda_{i(\mathbf{A}+\mathbf{C})}$ is, the shorter the synchronization time is.

5. Conclusions

In this paper, dynamics of the fractional-order simplified Lorenz hyperchaotic system are investigated based on the modified Adams-Bashforth-Moulton method. Chaotic range and periodic windows are determined by means of bifurcation diagrams, Poincaré sections, the largest Lyapunov exponent and phase portraits. Some typical bifurcations are observed, including interior crisis bifurcation, tangent bifurcation, pitchfork bifurcation and period-doubling bifurcation. It indicates that the fractional-order simplified Lorenz hyperchaotic system has rich dynamical behaviors, and the lowest order for this system to yield chaos is 3.8584. Moreover, synchronization between two identical fractional-order simplified Lorenz systems has been achieved via active control method. It is found that the synchronization time is decreasing with the increasing of q. Also, assuming that the sum of all the eigenvalues of the error system is same, the synchronization time decreases as the eigenvalues' standard deviation of the error system decreases. When all the eigenvalues are same, the synchronization time decreases with the eigenvalues decreasing. Next, our work is to study the applications of these two synchronized identical fractional-order simplified Lorenz systems.

Acknowledgements

The authors would like to thank the editor and the referees for their carefully reading of this manuscript and for their valuable suggestions.

References

[1] M. S. Abdelouahab, N. E. Hamri and J. W. Wang, *Hopf bifurcation and chaos in fractional-order modified hybrid optical system*, Nonlinear Dynamics, 69(2011), 275-284.

[2] W. M. Ahmad and J. C. Sprott, *Chaos in fractional-order autonomous nonlinear systems*, Chaos, Solitons & Fractals, 16(2003), 339-351.

[3] D. Y. Chen,R. F. Zhang and J. C. Sprott, *Synchronization between integer-order chaotic systems and a class of fractional-order chaotic systems via sliding mode control*, Chaos, 22(2012), 23130.

[4] M. A. Ezzat, A. S. El Karamany and M. A. Fayik, *Fractional order theory in thermoelastic solid with three-phase lag heat transfer*, Archive of Applied Mechanics, 82(2012), 557-572.

[5] J. W. Fan , N. Zhao and Y. Gao, *Function synchronization of the fractional-order chaotic system*, Advanced Materials Research, 631(2013), 1220-1225.

[6] C. Ionescu, J. T. Machado and D. R. Keyser, *Fractional-order impulse response of the respiratory system*, Mathematics with Applications, 62(2011), 845-854.

[7] M. Javidi and N. Nyamoradi, *Dynamic analysis of a fractional order phytoplankton model*, Journal of Applied Analysis and Computation, 3(2013), 343-355.

[8] E. Kaslik, S. Sivasundaram, *Nonlinear dynamics and chaos in fractional-order neural networks*, Neural Networks, 32(2011), 245-256.

[9] S. Kuntanapreeda, *Robust synchronization of fractional-order unified chaotic systems via linear control*, Computers & Mathematics with Applications, 63(2012), 183-190.

[10] E. T. McAdarns, A. Lackermeier and J. A. McLaughlin, *The linear and nonlinear electrical properties of the electrode-electrolyte interface*, Biosensors & Bioelectronics, 10(1995), 67-74.

[11] A. G. Radwan, K. Moaddy and K. N. Salama, et al., *Control and switching synchronization of fractional order chaotic systems using active control technique*, Journal of Advanced Research, 5(2014), 125-132.

[12] G. Q. Si , Z. Y. Sun and Y. B. Zhang, *Projective synchronization of different fractional-order chaotic systems with non-identical orders*, Nonlinear Analysis: Real World Applications, 13(2012), 1761-1771.

[13] K. H. Sun , Y. Wang and X. Liu, *Design and circuit implementation of hyperchaotic system based on linear feedback control*, Journal of Circuits and Systems, 18(2013), 500-504 (in Chinese).

[14] H. H. Sun, A. A. Abdelwahab and B. Onaral, *Linear approximation of transfer function with a pole of fractional power*, IEEE Transactions on Automatic Control, 29(1984), 441-444.

[15] V. E. Tarasov, *Fractional integro-differential equations for electromagnetic waves in dielectric media*, Theoretical and Mathematical Physics, 158(2009), 355-359.

[16] Y. Xu, R. C. Gu and H. Q. Zhang, *Chaos in diffusionless Lorenz system with a fractional order and its control*, International Journal of Bifurcation and Chaos, 22(2011), 12500884.

[17] R. Zhang and S. Yang, *Adaptive synchronization of fractional-order chaotic systems via a single driving variable*, Nonlinear Dynamics, 66(2011), 831-837.